UDC 620.192.63

FLAW DETECTION CONTROL SYSTEM OF CONDUCTIVE COATING OF AIRCRAFT FUEL TANKS AND ITS SIMULATION MODELING

B.V. Skvortsov, A.S. Samsonov, D.M. Zhivonosnovskaya

S.P. Korolyov Samara State University

34, Moskovskoye sh., Samara, 443086, Russian Federation

Abstract. *The conductive coating control method of the aircraft fuel tanks is discussed. Monitoring device construction and a general description of the scanning process are given. The effect of stray capacitance on the calculation error is made. The analytical equations describing the change in the capacitance between the conductive coating and scanning electrode are provided. A program of flaw detection of the modeling process simulating the passage of the scanning system over the fuel tank is developed. A maximum scanning velocity at given dynamic error is defined.*

Keywords: *fuel tank, conductive coating defects, control, capacitive method, sensor construction, simulation, dynamic error.*

The development of accurate on-line control of current-conducting coating (CCC) integrity for spacecraft fuel tanks is an important task for the safe operation, transportation, and maintenance of the tanks, especially when using cryogenic fuel. Tank surfaces are generally coated with dielectric heat insulation material, and the CCC is applied on top of the heat insulation to facilitate the discharge of static electricity. In accordance with GOST, the structural components on the outer surface of an item must be coated with metal when the item's surface area is above 0.2 m^2, or, when using hydrogen fuel, above 0.02 m^2 [1]. Because a coat of paint is applied on top of the CCC, visual and contact test methods of its integrity are difficult to perform. Closed cracks or spots without coating may develop on the CCC during operation, process re-laying, transportation, and maintenance. Static electricity charges accumulate at the defective areas, which can lead to inflammation in the case of fuel leakage or emission through pneumatic valves. In order to ensure the safety of the tank, the ground facilities, and the people working with it, careful monitoring of CCC integrity is required. The large overall dimensions of the tanks, which can amount to 15 × 3 m (length × diameter), generate additional difficulties for CCC diagnostics. The device will automatically omit defects in areas that do not exceed the set value $S_0 < 0.02$ m^2, which amounts to a linear square with 141 × 141 mm dimensions.

In [2], various CCC types and a classification of their defects are described. Their defects can take the form of either closed cracks or an absence of coating and can be completely or partially covered with the outer paint coat. In [3], a summary of methods and devices for non-destructive testing of different CCC types is given, and it is concluded that the known x-ray, ultrasonic, magnetic, and eddy-current methods are significantly limited, especially when testing multilayer large-scale tanks. For instance, fluctuation of the CCC film thickness on aircraft tanks generally amounts to 0.05–0.1 mm, and these large errors make it impossible to use eddy-current methods effectively, as measurements of CCC thickness and uniformity are critical for eddy-current methods. Furthermore, eddy-current methods record all defects, increasing the test time in a manner not reasonable for resolution of the task under discussion.

Boris V. Skvortsov (Dr. Sci. (Techn.)), Professor.
Alexander S. Samsonov, Postgraduate Student.
Driya M. Zhivonosnovskaya, Engineer.

A device protected with patent [4] has been developed, which implements a capacitance test method for testing CCC integrity (Fig. 1). In the functioning of this device, an electrode (3) is moved by a platform (2) along the CCC (8), and the gap is monitored by a sensor (6). The platform is moved by means of a control and processing device (4), which receives a signal from the electrode proportional to the valid values of condenser capacity determined by the electrode and the CCC. It also receives signals from the sensor (6) proportional to its distance from the sensor. Recorded capacity values C_{val} are continuously compared with the reference capacity value C_r by the processing device, and the difference is calculated as $\Delta C_{val} = C_r - C_{val}$. The defect tagging device (5) marks defective areas on the protective coating surface (7) based on signals it receives from the processing device. These signals are sent when the inequation $\Delta C_{val} \geq \Delta C_{all}$ is met, where ΔC_{all} is the maximum allowable value of ΔC_{val}, selected based on the device sensitivity. The proposed invention allows increasing accuracy of monitoring by means of its air gap sensor. In the diagram shown in Fig. 1, (9) is the defective spot of CCC, and (10) is the heat insulation.

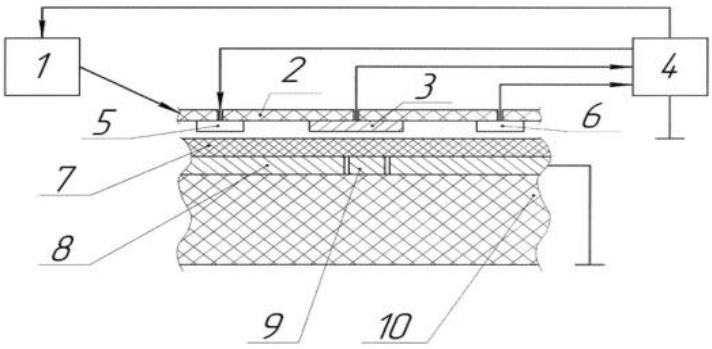

Fig. 1 CCC monitoring device

In the general case, the total sensor current depends on the defect area and the structural parameters of the generalized function:

$$\dot{I} = F(S_\partial, d_k, \sigma_k, \varepsilon_k, \omega, U_m) = A(S_\partial, d_k, \sigma_k, \varepsilon_k, \omega, U_m) e^{j\phi(S_\partial, d_k, \sigma_k, \varepsilon_k, \omega, U_m)}. \quad (1)$$

Here, S_∂ is the defect area, d_k is the thickness of each layer, σ_k, ε_k are the conductivity and dielectric capacitivity of each layer, respectively, and ω, U_m are the sensor power supply frequency and voltage, respectively.

The entire monitoring process is illustrated in Fig. 2, according to which the platform (2) is moved along the surface by means of a special coordinate-positioning device controlled by an electric drive (8) via the position sensor (9).

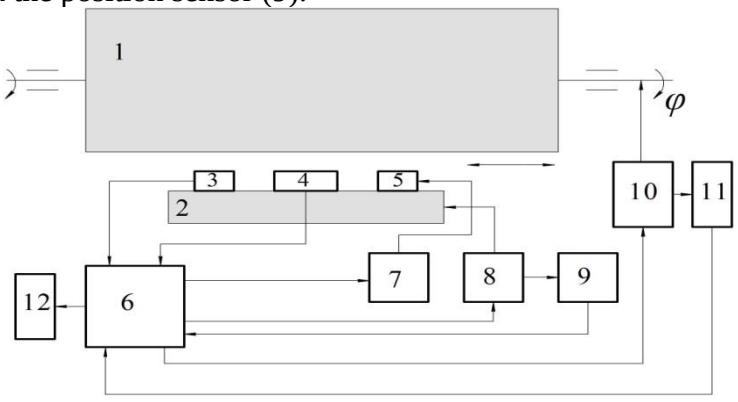

Fig. 2 Structural diagram of the fuel tank CCC monitoring system. 1 – fuel tank; 2 – scanning platform; 3 – gap sensor; 4 – capacity sensor (scanning electrode); 5 – nozzle; 6 – control block; 7 – cartridge control device; 8 – platform electric drive; 9 – position sensor; 10 – tank turning electric drive; 11 – turn angle sensor; 12 – computer

When the sensor has moved the entire length of the tank, the tank is turned with an electric drive (10) at a fixed angle determined by the electrode size, and the scan is repeated. If a defect is detected under the electrode, the nozzle makes a line on the tank along the scanning path corresponding to the length of the defect.

Calculations based on the electric field analysis in the sensor structure are shown in Fig. 1. With regard to their dispersion, it was demonstrated that defects have little effect on conductivity, while the sensor capacity significantly depends on the size of the defects. A diagram of the capacity change when the electrode is moved under a closed crack is shown in Fig. 3.

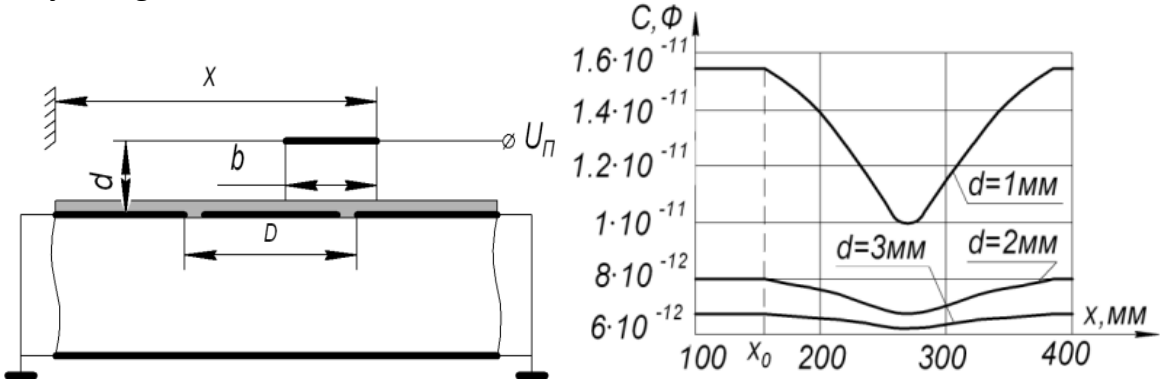

а *б*

Fig. 3 Sensor capacity change during electrode movement over a defect at b = 100 mm and D = 140 mm. b – electrode width; d – air gap; D – defect size; x_0 – initial defect coordinate

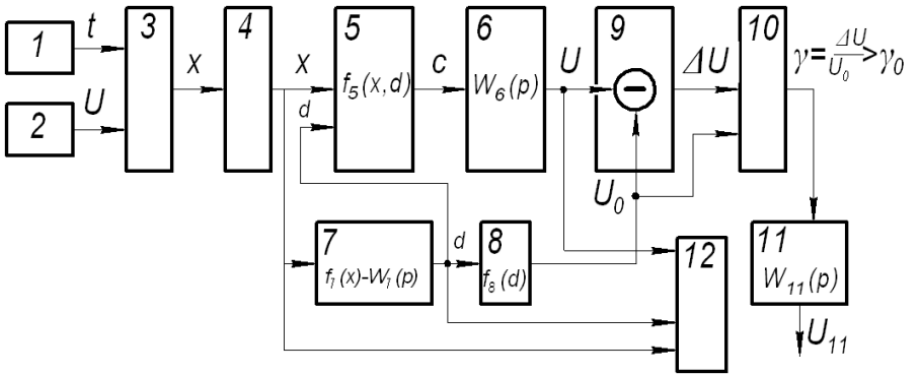

Fig. 4 Functional diagram of CCC monitoring process modeling program. 1 and 2 – the time and speed setting blocks; 3 – multiplication block; 4 – stop subsystem; 5 – capacity sensor; 6 – capacity conversion link; 7 – gap sensor; 8 – support signal generation link; 9 – comparator; 10 – processing device; 11 – nozzle control device; 12 – recording block

An assessment of effect of the stay capacitance on the sensor information signal has been provided based on calculations and analytical examinations in [5]. The relative value of the stay capacitance C_S can be determined as follows:

$$\gamma = \frac{C_{П}}{C_0} = \frac{0,005[\ln(\frac{8\pi b}{d_B + d_Л}) - 3]}{b}(\frac{d_B}{\varepsilon_B} + \frac{d_Л}{\varepsilon_Л}). \quad (2)$$

Here, d_V and d_L are the thickness and dielectric capacitivity of the air, respectively, while ε_V and ε_L are those of the paint coat.

Equation (2) allows for the selection of such values of electrode width b and air gap thickness d_V at which the dispersion field can be neglected given the set error. At such conditions, the conversion function shown in Fig. 3*b* can be described analytically [6]:

$$C(x) = C_1 + C_2 + C_3, \quad (3)$$

At $x \le x_0$ $C_1 = \varepsilon_0 \frac{b^2}{A}$, $C_2 = 0$, $C_3 = 0$; $A = \frac{d_в}{\varepsilon_в} + \frac{d_л}{\varepsilon_л}$, $B = \frac{d_П}{\varepsilon_П} + \frac{d_T}{\varepsilon_T}$;

At $x_0 \le x \le x_0 + b$ $C_1 = \varepsilon_0 \frac{b(b - x + x_0)}{A}$, $C_2 = \varepsilon_0 \frac{b(x - x_0)}{A + B}$, $C_3 = 0$;

At $x_0 + b \le x \le x_0 + D$ $C_1 = 0$, $C_2 = \varepsilon_0 \frac{b^2}{A + B}$, $C_3 = 0$;

At $x_0 + D \le x \le x_0 + b + D$ $C_1 = 0$, $C_2 = \varepsilon_0 \frac{b(b - x + x_0 + D)}{A + B}$, $C_3 = \varepsilon_0 \frac{b(x - x_0 - D)}{A}$;

At $x \ge x_0 + b + D$ $C_1 = 0$, $C_2 = 0$, $C_3 = \varepsilon_0 \frac{b^2}{A}$.

The tentative mathematical model in Eq. (3) approximates the diagram shown in Fig. 3b with straight-line segments with error $\gamma < 1\%$, indicating that its theoretical statements are valid.

The diagram shown in Fig. 3*b* illustrates the conversion function of the capacity sensor $C(x)$ at a scanning speed much lower than the speed of the inertia processes shown in the signal processing diagram. Scanning speed is the most important parameter affecting the information signals in the monitoring procedure.

A program in a MATLAB/Simulink environment that allows for the modeling of non-destructive testing procedures was developed. The program imitates signals that describe the movement of the platform that contains the electrode, the air gap sensor, and the paint cartridge above the tank surface. When the metering system passes above an area with a defect, the capacity between the electrode and the CCC is reduced (Fig. 3*b*), and the system marks the defective area of the tank with paint. A functional diagram of the model is presented in Fig. 4. After startup, block 1 begins modeling the time. The signal from block 1 is sent to blocks 2 and 3 simultaneously. Block 2 contains the data array describing the measurement of the speed relative to the time, while block 3 multiplies the speed and time parameters. Thus, the original coordinate of the electrode x is the output of block 3, and this signal is sent to subsystem 4, which stops the scanning when the electrode reaches the platform edge. In the case that the conditions for continuation of the model are met, the signal of the electrode coordinate, having changed over time, is sent to subsystems 5 and 7. These model the operation of the defect capacity sensor and the gap sensor, respectively.

The table function $F_5(x, d)$ is set in block 5 as the law of capacity change, which depends on the coordinate x and the gap d. This function models the defect position, which is as depicted in Fig. 3a. In the case that no defect is found, $F_5(x, d) = Const$, and the transfer function $W_6(p) = k_6/(T_6 p + 1)$ are described in an electrical signal via the dynamic capacity conversion link. In block 7, the gap change of the coordinate is set by the table function $F_7(x)$, the value of which is converted via the dynamic link to an electrical signal with the transfer function $W_7(p) = k_7/(T_7 p + 1)$. The function $F_7(x)$ models the surface bends relative to the reference value, where, in the perfect

case, $F_7(x) = Const$. The function $F_8(d)$ is modeled in the support signal (U_0) generation link and demonstrates the way the signal reference value should be corrected when the gap is changed so that its value is not recognized as a defect at $d = Const$ or $F_8(d) = Const$. The comparator deducts the signals corresponding to the current and reference values for the current gap of the capacity sensor via the equation $\Delta U = U_0 - U$. The processing device calculates and analyzes the relative deviation ε, and when $\gamma > \gamma_0$, it sends a signal to the nozzle, which makes a note of the defect. The nozzle control device is modeled according to the delay link $W_{11}(p) = e^{-p\tau}$. The recording block records the values of the capacity and the gap depending on the surface coordinate according to the protocol. The developed model allows the device to make examinations in which the following parameters can be varied: platform movement speed; surface roughness; defects in the CCC; and response delay of the sensors and the actuator. The scanning speed and the effect of the sensors' time constants on the information signals and coordinate determination errors were examined, and the results are presented in Fig. 5.

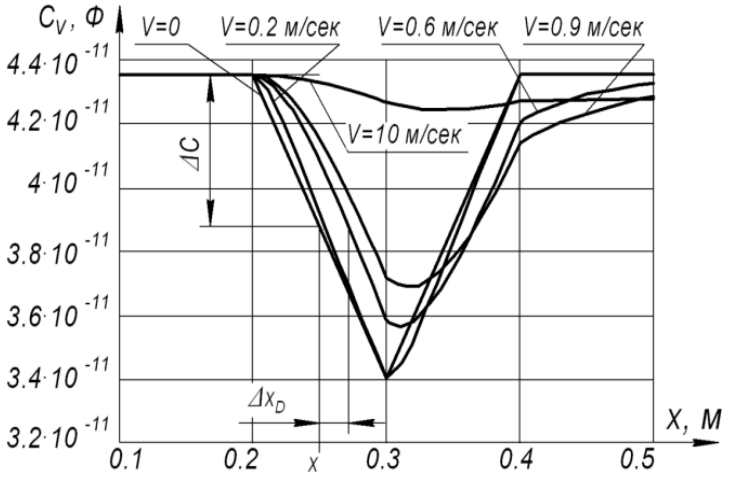

Fig. 5 Capacity change at different scanning speeds. $D = b$; $T = T_6 = T_7 = 0.1$ s

The diagram shown in Fig. 5 demonstrates that increasing the scanning speed or the time constants of the sensors, T, results in a decrease in the amplitude of the defect signal and a shift in the direction of scanning. When the speed V and the time constants of the links T are increased, the minimum capacity value is decreased, which affects the ability to detect the defect on the tank surface. These increases also cause a shift in the coordinate of the defect center. At $V \to \infty$ or $T \to \infty$, the difference between the maximum and minimum capacity values tends to be 0 ($(\Delta C_0 = C_{MAX} - C_{MIN}) \to 0$). At the selected threshold ΔC and with any values of V and T there arises a situation in which the electrode misses a defect, as the capacity is not able to change to a value larger than the threshold value ΔC. A formula describing the relationship between scanning speed, allowable dynamic error $\Delta x_Д$, and the sensor's structural parameters can be expressed as follows:

$$V = \frac{\Delta C(\mathrm{A}+\mathrm{B}) - b\varepsilon_0 \Delta x_Д}{b\varepsilon_0 T \cdot \ln[1 - \frac{\Delta C(\mathrm{A}+\mathrm{B})}{\Delta C(\mathrm{A}+\mathrm{B}) - b\varepsilon_0 \Delta x_Д}]}. \quad (4)$$

Formula (4) is valid at $x_0 < x < x_0 + b$, where according to the set error $\Delta x_Д$ and the known structural parameters, the scanning speed limit can be obtained. A diagram of scanning speed change depending on dynamic error at different T values is shown in Fig. 6.

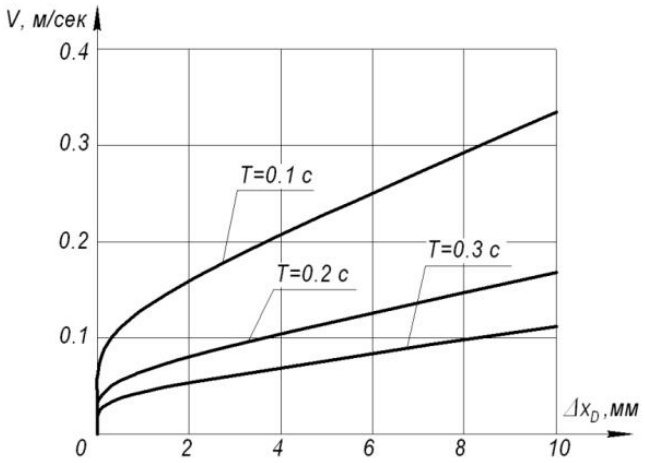

Fig. 6 Diagram of scanning speed limit determination with the set dynamic error

Modeling and data analysis demonstrated that the device was able to make a mark within the defect location set by block 5 on Fig. 4, and that the results did not depend on gap changes. The developed simulation model allows for a dynamic examination of the effect of numerous structural and schematic parameters on the accuracy of defect identification. It also allows for the optimization of parameter selection and scanning mode.

REFERENCES

1. *Каргин Н.Т., Волоцуев В.В.* Конструкция и проектирование изделий ракетно-космической техники. Ч. 1. Конструирование изделий ракетно-космической техники: электрон. учеб. пособие. – Самара, 2012. – 1 эл. опт. диск (CD-ROM).
2. *Самсонов А.С., Скворцов Б.В.* Контроль целостности токопроводящего покрытия топливных баков летательных аппаратов // Авиакосмическое приборостроение. – 2015. – № 9. – С. 34–40.
3. *Скворцов Б.В., Самсонов А.С., Блинов Д.И.* Проблемы дефектоскопического контроля токопроводящего покрытия топливных баков летательных аппаратов // Известия СНЦ РАН. – 2016. – № 9. – С. 34–40.
4. Пат. 159780 Российская Федерация, МПК G01N27/24. Устройство контроля целостности токопроводящего покрытия на диэлектрическом материале / *Б.В. Скворцов, А.С. Самсонов, Д.И. Блинов*. – № 2015154359/28; заявл. 17.12.15; опубл. 20.02.16, Бюл. № 5. – 2 с.
5. *Мишин А.И.* Математическое моделирование процессов рассеяния энергии в тонкопленочных электролюминесцентных конденсаторах: Дис. … канд. техн. наук. – Ульяновск, 2007. – 106 с.
6. *Батищев В.И., Мелентьев В.С.* Измерение параметров емкостных датчиков положения и перемещения. – М: Машиностроение-1, 2005. – 124 с.

Article submitted 1 April 2016.

СИСТЕМА ДЕФЕКТОСКОПИЧЕСКОГО КОНТРОЛЯ ТОКОПРОВОДЯЩЕГО ПОКРЫТИЯ ТОПЛИВНЫХ БАКОВ ЛЕТАТЕЛЬНЫХ АППАРАТОВ И ЕЕ ИМИТАЦИОННОЕ МОДЕЛИРОВАНИЕ

Б.В. Скворцов, А.С. Самсонов, Д.М. Живоносновская

Самарский национальный исследовательский университет имени академика С.П. Королёва

Россия, 443086, г. Самара, Московское ш., 34

Аннотация. *Рассматривается метод контроля токопроводящего покрытия (ТПП) топливных баков летательных аппаратов. Дана конструкция устройства контроля ТПП и общее описание процесса сканирования. Произведена оценка влияния паразитной емкости на погрешность расчета. Приведены аналитические выражения, описывающие изменение емкости между ТПП и сканирующим электродом. Разработана программа моделирования процесса дефектоскопии, имитирующая проход сканирующей системы над топливным баком. Проведено исследование влияния скорости передвижения сканирующей платформы на погрешность контроля. Определена максимально допустимая скорость сканирования при заданной динамической погрешности.*

Ключевые слова: *топливный бак, токопроводящее покрытие, дефекты, контроль, емкостной метод, конструкция датчика, моделирование, динамическая погрешность.*

Борис Владимирович Скворцов (д.т.н., проф.), научный руководитель НИЛ «Аналитические приборы и системы».

Александр Сергеевич Самсонов, аспирант.

Дарья Михайловна Живоносновская, инженер НИЛ «Аналитические приборы и системы».